

Destruction of classical cantori in the quantum Frenkel-Kontorova model

F. Borgonovi^{1,2}, I. Guarneri¹, and D. Shepelyansky²

¹ Dipartimento di Fisica Nucleare e Teorica dell'Università di Pavia, and Istituto Nazionale di Fisica Nucleare, Pavia, Italy

² Institute of Nuclear Physics, Novosibirsk, USSR

Received September 25, 1989

In this paper we investigate the properties of the quantized discrete Frenkel-Kontorova model. The structure of the ground state is numerically analyzed by means of the Metropolis algorithm; special attention is given to the effects of quantization on the Cantori structure of the classical ground state. These quantum effects produce a new structure which can be approximately described by using a sawtooth map instead of the Standard map. The dependence of the quantum energy on temperature is also investigated and discussed in connection with these structural modifications.

1. Introduction

The understanding of the correspondence between quantum and classical mechanics for nearly integrable systems is a subject of considerable interest [1]. Following the highlights of the Kolmogorov-Arnol'd-Moser theorem, an effectual combination of mathematical skill and sophisticated computer performances has been revealing in more and more detail the process of destruction of invariant surfaces that takes place when a classical integrable system is subjected to a perturbation of increasing strength. It is now known that after the breakup of certain invariant surfaces (tori), some relics may be left in the form of invariant Cantor sets, which are named Cantori [2, 3, 4].

Now the necessity arises of understanding the quantum relevance of such intriguing classical results. Increasing efforts are devoted to the investigation of the effect of classical Cantori on the structure of quantum wave functions [5, 6]. Up to now, only dynamical models have been considered, i.e. models describing the evolution in time of some physical system. However, Cantori can be relevant also for static properties of many-particle systems. A well known example from Solid State Physics is the discrete Frenkel-Kontorova model (FK) [3, 4, 7].

The classical version of this model has attracted much attention because of the unusual properties of its ground state. A rigorous mathematical analysis has shown that the configuration of the (properly defined) classical ground state is determined by certain invariant sets of the Standard map, which can be tori or Cantori according to whether the parameter of the map is smaller or larger than a critical value.

This transition involves a deep change in the structure of the ground state and is accompanied by a number of physically relevant phenomena, such as the appearance of a *phonon gap*. It is therefore important to investigate to what extent such classical predictions survive in the more realistic quantum domain. To the best of our knowledge, only a few attempts have been made at theoretically investigating this problem [7, 8, 9] and very little is known, because the high nonlinearity of the model renders a mathematical analysis very difficult.

In this paper we present the first numerical results on the structure of the quantum ground state (some of these results were anticipated in [10]). In our simulations we used the Metropolis algorithm [11, 12] for computing Feynman-Kac integrals. In Sect. 2 some basic facts about the FK model are briefly reviewed and the numerical methods of our quantum simulation are described. In Sect. 3 the classical and quantum numerical results are discussed.

Finally, Sect. 4 is devoted to some results on the quantum thermodynamics of the model, which illustrate the dependence of the energy on the temperature.

2. Model and numerical method

The discrete Frenkel-Kontorova model is an infinite linear chain of linearly coupled oscillators, in an external periodic potential. It is defined by the Hamiltonian:

$$H = T + V = \sum_i \left[\frac{1}{2} P_i^2 + \frac{1}{2} (x_i - x_{i-1})^2 - K \cos(x_i) \right] \quad (2.1)$$

where we have taken the mass of the particles and the elastic constant equal to one. The abscissae x_i of the particles in the equilibrium configuration must satisfy the condition:

$$\frac{\partial V}{\partial x_i} = x_{i+1} + 2x_i - x_{i-1} + K \sin(x_i) = 0. \quad (2.2)$$

Upon introducing new variables $p_{i+1} = x_{i+1} - x_i$ the condition can be written in the form of an area-preserving map

$$\begin{aligned} p_{i+1} &= p_i + K \sin(x_i) \\ x_{i+1} &= x_i + p_{i+1} \end{aligned} \quad (2.3)$$

which becomes the well known Standard map [13] as soon as the variables x_i are taken *modulo* 2π .

If a fixed density is assumed for the infinite chain, then the equilibrium configuration corresponds to an orbit of the Standard map with a given rotation number ν . In our investigations we used a finite chain of s oscillators, with a given length $2\pi r$ and fixed boundary conditions. This amounts to approximating the true infinite orbit with rotation number ν by means of periodic orbits with rational rotation numbers $\nu_s = r/s$. This kind of approximation is frequently used in numerical investigations of the breakup of KAM curves [14]. In our case, we have taken for ν_s the rational approximants of the

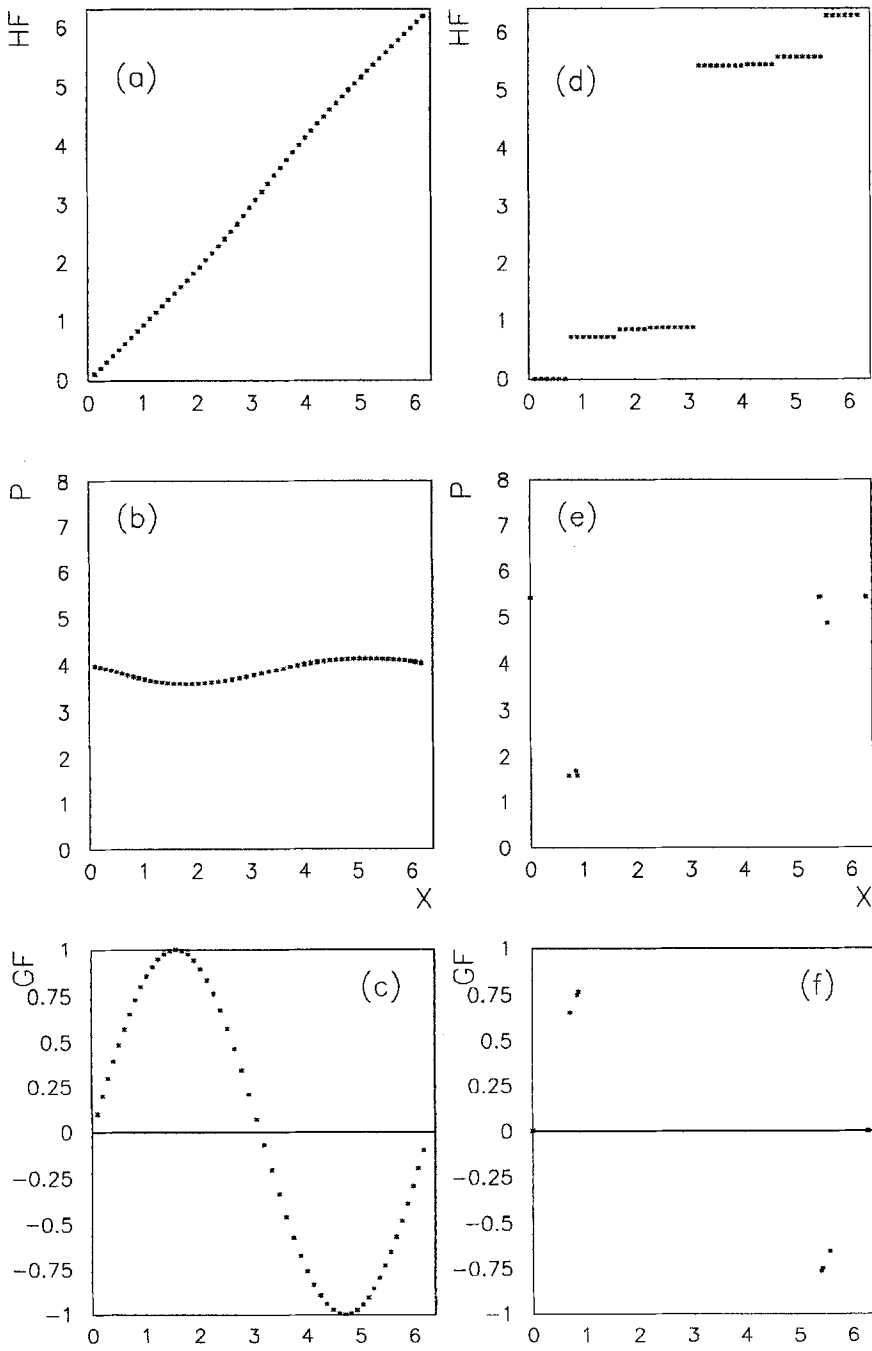


Fig. 1a-f. Structure of the classical ground state and transition by breaking of analyticity ($\nu = 34/55$). On the left column $K = 0.5$, on the right $K = 5$. **a** and **d**: the dependence of the hull function on the unperturbed positions of the atoms $il(\text{mod } 2\pi)$, **b** and **e**: plot in the space (x, p) of the Standard map, **c** and **f**: g -functions

golden mean $(\sqrt{5}-1)/2$, as provided by a continued fraction expansion. This choice is motivated by well-known results of the KAM theory for the Standard map: for irrational ν and K small enough, there is an invariant torus (a KAM curve) of the Standard map, with rotation number ν . These KAM curves break at some critical value K_{cr} of K ; in their places, invariant Cantor sets named Cantori are left. The last KAM curve undergoing this fate corresponds to the *most irrational* rotation number $\nu=(\sqrt{5}-1)/2$; its breakdown occurs at $K_{cr}=0.971635\dots$ [14, 15]. The bulk of our classical and quantum computations were made with $r=34$, $s=55$; however, also additional checks with $r=233$, $s=377$ were performed.

The breakup of the invariant tori of the Standard map has a counterpart in the FK model; indeed at $K=K_{cr}$ an abrupt change occurs in the nature and properties of ground state of that model. This transition was investigated by Aubry [3, 4] and is known as a “transition by breaking of analyticity”, for the following reason. Let $u_i=x_i(\text{mod } 2\pi)$ and let $l=2\pi\nu$ the average distance between neighbouring oscillators. Then a function f is proven to exist, such that, for any i ,

$$u_i = f((il + \alpha) \text{ mod } 2\pi) \quad (2.4)$$

where α is an appropriate phase. This f is called a “hull function”. For $K < K_{cr}$ it is a monotonic analytic function, and for $K > K_{cr}$ it is a monotonic function with a countable set of step discontinuities. The stepwise character of f for $K > K_{cr}$ reflects the presence of Cantori in the Standard map, and shows that the ground state of the FK model is never chaotic.

The transition by breaking of analyticity is accompanied by a number of physically relevant manifestations. Of particular relevance to the present work is the appearance of a gap in the “phonon spectrum” [16] – i.e., the spectrum of frequencies of small oscillations around the equilibrium configuration.

The above sketched classical phenomenology is illustrated by the numerical results shown in Fig. 1, which provide a term of comparison for the quantum results to be discussed below. In order to compute the equilibrium positions of the classical model we exploited the gradient method described in [16]. The left and the right columns in Fig. 1 refer to values of $K=0.5$ (subcritical) and $K=5$ (overcritical) respectively. Besides the hull functions (1a, 1d), we show pictures of the points $x_i, p_i (=x_i - x_{i-1})$ in the phase space of the Standard map (not to be confused with the phase space of the FK model). Moreover we present a plot of the values g_i , defined

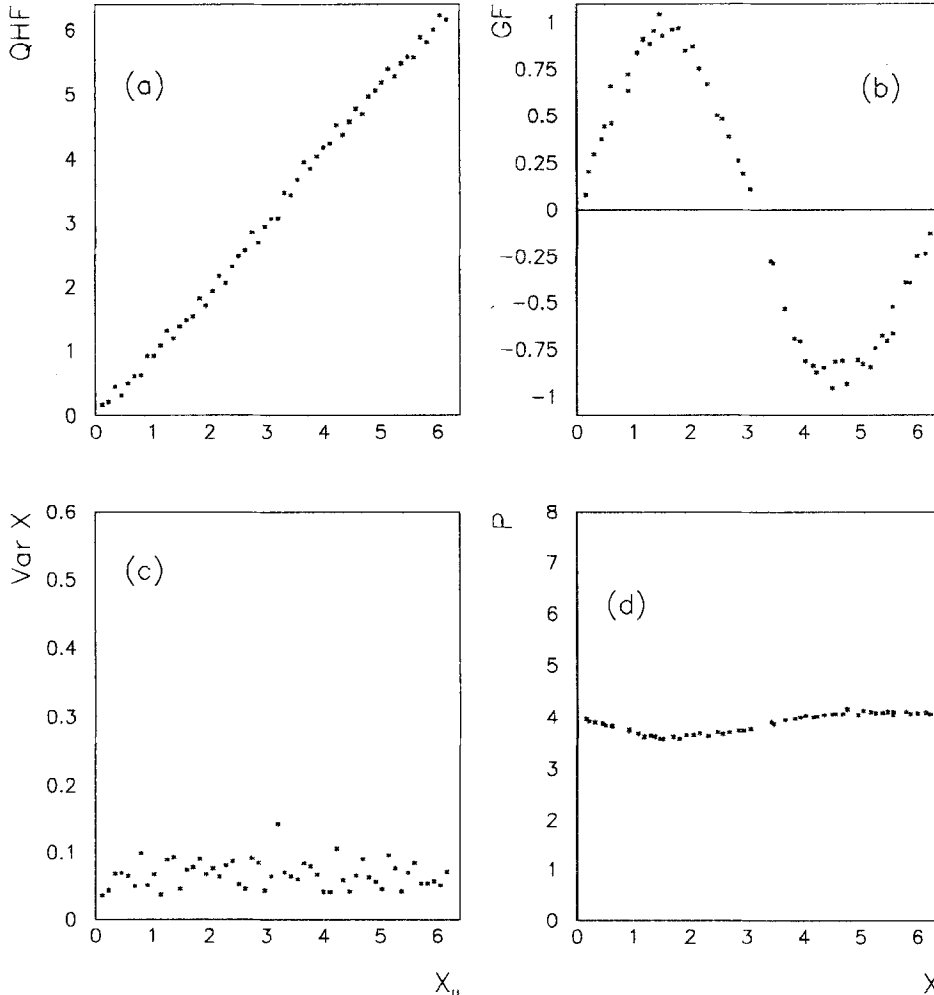


Fig. 2a–d. Structure of the quantum ground state in the undercritical case for $\hbar=0.2$, $T=0.0067$, $K=0.5$, and $\nu=34/55$. **a** Quantum hull function; **b** Quantum g -function; **c** Variances of positions against unperturbed positions $x_u(\text{mod } 2\pi)$; **d** plot in the phase space of the Standard map

by

$$g_i = \frac{x_{i+1} - 2x_i + x_{i-1}}{K} \tag{2.5}$$

versus the values x_i . As is apparent from (2.3) the points thus obtained must belong in the graph of the function $g(x) = \sin(x)$; actually in the overcritical case they belong in a Cantor subset of that graph.

The Hamiltonian (2.1) depends on $(s-1)$ configuration variables $x_j, j=2, \dots, s, (x_1=0, x_{s+1}=2\pi r)$. For numerically investigating the ground state of the quantum model we used a well known method [11, 12], based on Feynman quantization. In the Feynman approach the quantum propagator between states $|x_i\rangle$ and $|x_f\rangle$ from time 0 up to time t is given by

$$\langle x_f | e^{-iHt/\hbar} | x_i \rangle \simeq \int [dq] e^{\frac{i}{\hbar} S[q]} \tag{2.6}$$

where x denote vectors of positions $x_j, 2 \leq j \leq s$ and $S[q]$ is the classical action of a path which starts from $|x_i\rangle$ at time 0 and reaches $|x_f\rangle$ at time t . The formal integral $\int [dq]$ means the sum over all such paths.

Upon going over to the euclidean time $\tau = it$, one gets the euclidean propagator:

$$\langle x_f | e^{-\tau H/\hbar} | x_i \rangle = \sum_{n=0}^{\infty} \Psi_n^*(x_f) \Psi_n(x_i) e^{-\tau E_n/\hbar} \tag{2.7}$$

with $\Psi_n(x), E_n$ the energy eigenfunctions and eigenvalues of the Hamiltonian. In the Feynman-Kac formulation this propagator can be found by averaging over all classical paths weighted by the Boltzmann factor $e^{-\tau S/\hbar}$ where S is now the euclidean action. According to (2.7) this average yields quantum thermodynamical averages [11, 12] with the parameter \hbar/τ playing the role of temperature. Nevertheless, if τ/\hbar is large enough the ground state contribution dominates in formula (2.7) and the ground state expectation value of any observable can be computed as an average over such a Boltzmann distributed ensemble of paths.

In order to numerically compute such an ensemble average we discretized the path with a suitable time step and we exploited the Metropolis algorithm [11, 12]. This method performs an "importance sampling" by randomly generating a finite set of paths which mainly contribute in the Feynman-Kac integral. The number of paths in the randomly generated sample determines the convergence of the finite-sample statistics, and it must be large enough for the fluctuations to be acceptably small. The actual number of steps required for that depends on the time step, which in turn must be large enough to isolate the ground state contribution. We used 300-1000 time steps and ensembles of 2000-8000 paths. The whole algo-

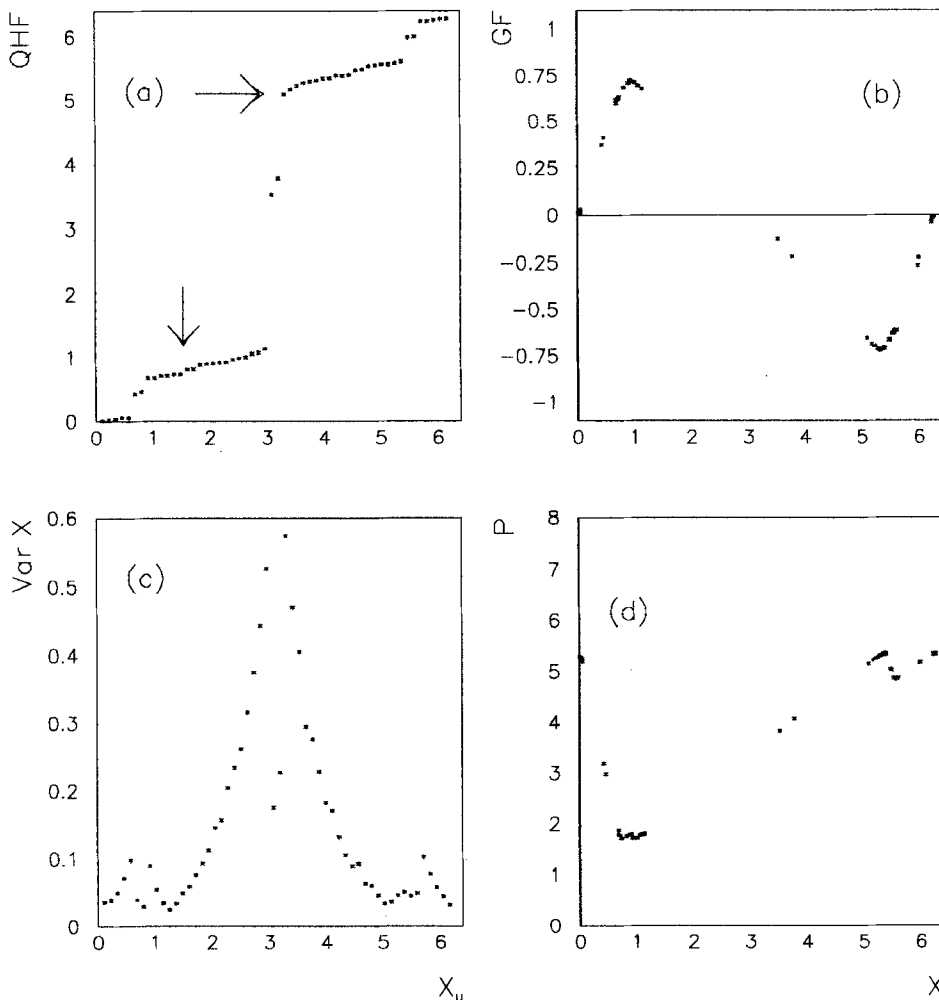


Fig. 3a-d. Same as Fig. 2 in the overcritical case for $K=5$

rithm was adjusted by working out the case $K=0$ for which exact analytical results are available; the final agreement between exact and Metropolis data was good.

3. Numerical results on the quantum model

The above described numerical approach was used to investigate the properties of the ground state of the quantum FK model. The expectation values $\langle x_j \rangle$ ($j=2, s$) of the positions of the oscillators at negligibly small temperature $T=\hbar\tau^{-1}$ computed by the Metropolis algorithm were used to construct the quantum analogues of Fig. 1.

In order to check that the obtained results describe the actual ground state structure and not just some temperature effects, we increased or decreased the temperature in a few times; in no case significant changes were observed. Moreover, from the study of thermal effects in the quantum model (Sect. 4) we got some quantitative information about the temperature required for significant excitation above the ground state. This temperature is measured by the plateau in Fig. 8. The temperatures in our ground state simulations were much smaller than that.

First of all, “quantum hull functions” (QHF) were produced by plotting the ground state average positions $\langle x_i \rangle \pmod{2\pi}$ against the unperturbed ones $\langle x_i \rangle \pmod{2\pi}$. As discussed above, in the classical case this procedure yields a set of points in the square $[0, 2\pi] \times [0, 2\pi]$, which belongs in the graph of the “hull function”. It is by no means obvious that the set of points obtained from quantum data should belong in the graph of a function whatsoever. Nevertheless, this kind of a plot allows for a straightforward pictorial comparison of quantum and classical data, and we loosely call it a “quantum hull function” for the sake of simplicity.

Besides that, from the quantum expectations $\langle x_i \rangle$ we computed the “momenta” $\langle p_i \rangle = \langle x_i \rangle - \langle x_{i-1} \rangle$, which were used to construct a phase space picture to be compared with Fig. 1 b, e.

Finally, we computed the values g_i according to (2.5) with $\langle x_i \rangle$ in place of x_i ; a plot of the g_i versus $\langle x_i \rangle$ yields a quantum counterpart for Figs. 1 c, f. Such a plot we call a “ g -function” (GF), though this denomination may be abusive on strict mathematical grounds.

Examples of such quantum results, below and above the critical value of K and for a small value of \hbar are shown in Figs. 2, 3. A comparison of these figures with their classical analogues (Fig. 1) shows that for small \hbar the quantum average positions approximately follow the classical ones. In particular, the classical transition is mirrored by a crossover in the nature of the QHF. Indeed, in the overcritical regime, the QHF has a step-like character, reminding of the classical hull function.

Nevertheless, a closer analysis revealed remarkable deviations from the classical behaviour in the overcritical regime. A first hint on the nature of these quantum effects was provided by the analysis of the variances of the positions of the oscillators. This is shown in Fig. 3 c, which is a plot of the mean-square deviations of the oscillators from their average positions:

$$\Delta x_j = \left[\frac{1}{N} \sum_{k=1}^N (x_j^k - \langle x_j \rangle)^2 \right]^{1/2}$$

here k labels the Metropolis paths, and N is the number of paths. In Fig. 3 c we observe a strong correlation between oscillators which belong to the same plateau in the hull function. The largest variances are given by oscillators which are located near the edge of a gap. This is explained by quantum tunneling; the quantum system is resonating between different configurations, in which the oscillators close to the edges of a gap belong to opposite sides of the gap itself. Such a picture was confirmed by the analysis of the probability distribution for the positions of the oscillators (Fig. 4). Oscillators near the edge of a gap have a double peaked distribution, with peaks corresponding to opposite edges of the gap itself.

The most interesting illustration of the effect of quantum fluctuations was provided by the quantum phase

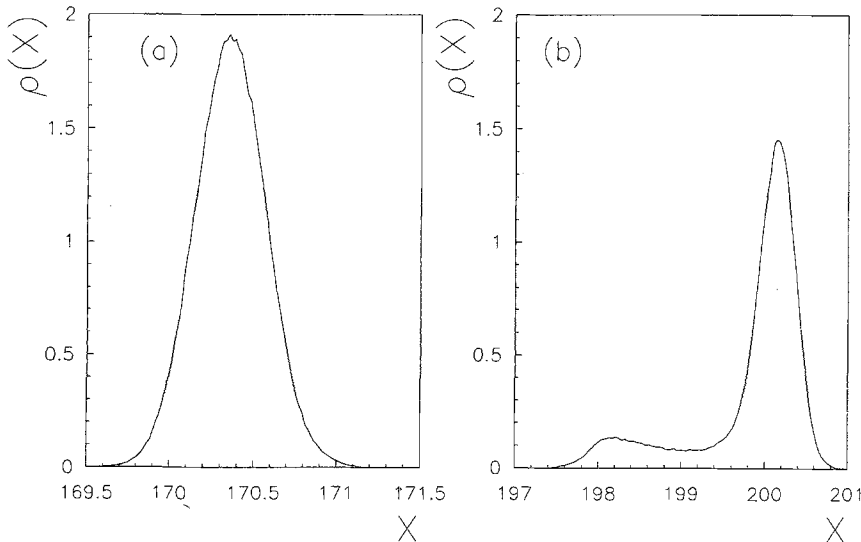


Fig. 4a, b. The probability density $\rho(x)$ of a the oscillator with a small variance singled out by the vertical arrow in Fig. 3 a, **b** the oscillator with a big variance indicated by the horizontal arrow in Fig. 3 a. The x -coordinate is measured from the left hand end of the chain (with the chosen units the area under the curve is equal to 1). Parameter values are as in Fig. 3

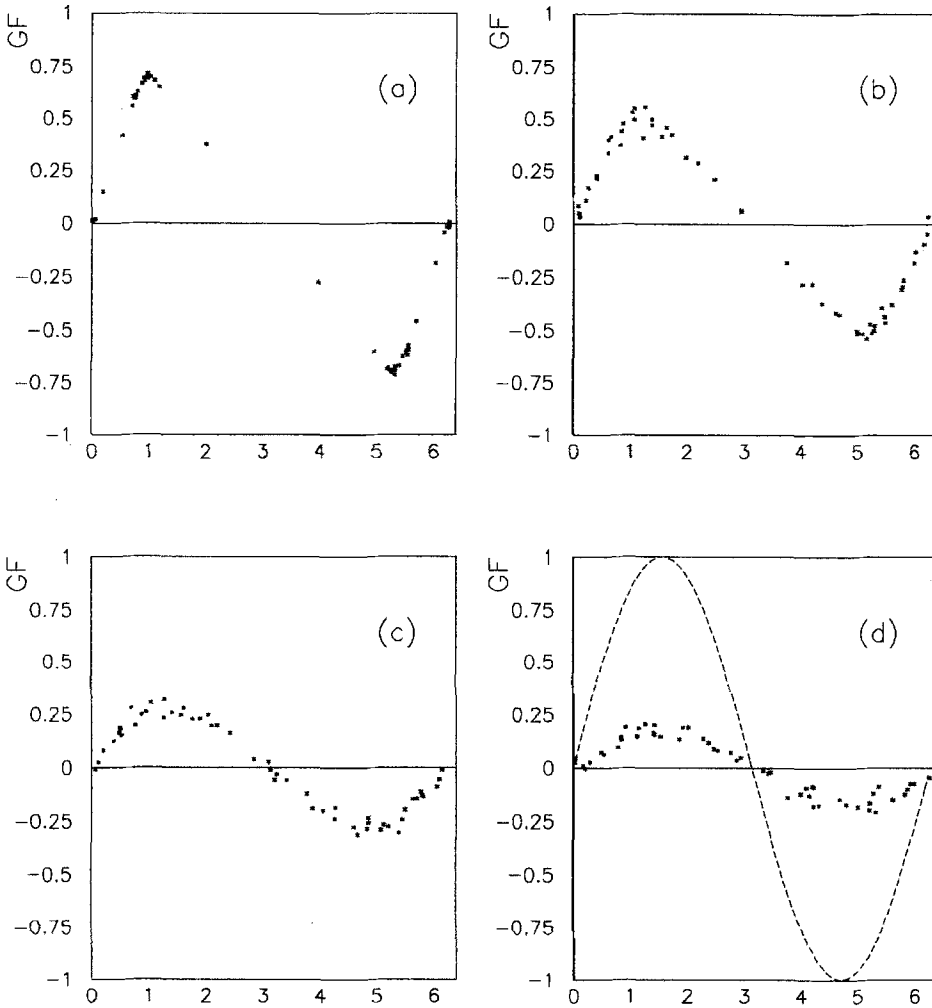


Fig. 5a-d. Variation of Quantum g -function with \hbar for $\nu=34/55$, $K=5$. **a** $\hbar=1$; **b** $\hbar=3$; **c** $\hbar=5$; **d** $\hbar=7$; the dashed line corresponds to the classical g -function $g(x)=\sin(x)$

space picture (Fig. 3d) and by the quantum GF (Fig. 5). The comparison of the classical phase picture (1e) with the quantum one (3d) shows that the quantum points spread out of the classical Cantorus, along straight lines that connect the edges of the gaps. As a result, a new object is formed, which we call a *quantorus*.

A similar tendency to fill the convex envelope of the classical Cantor structure is revealed by the analysis of the quantum GF (Fig. 5) for several values of \hbar . The points of the quantum GF are not concentrated in a small Cantor-like set (as they would classically) but appear to be more smoothly distributed. Surprisingly enough, even for large \hbar the points do not spread in the plane but follow a well defined curve, which is different from the classical $g(x)=\sin(x)$ and is close to a continuous sawtooth curve especially for $\hbar < 4$ (for $K=5$).

The indications provided by Figs. 3 and 5 yield qualitative but nevertheless definite evidence that quantum effects in the FK model tend to reduce the gaps in the classical structures. One may even be tempted to say that the quantum structures look more like KAM curves than the classical ones; though, of course, the blurring due to fluctuations makes it meaningless to speak about invariant curves or Cantori in the strict mathematical sense.

The nature of the quantum GF suggests that the quantum ground state configuration is better described by a sawtooth map than by the Standard map. Following this idea, we fitted the quantum GF by a continuous sawtooth function:

$$g(x) = \begin{cases} cx & 0 < x < x_0 \\ a(\pi - x) & x_0 \leq x \leq 2\pi - x_0 \\ c(x - 2\pi) & 2\pi - x_0 < x < 2\pi \end{cases} \quad (3.1)$$

where $a=(cx_0)/(\pi-x_0)$ and the parameters c , x_0 were obtained from the quantum numerical data. Then we studied the dependence of the fitting parameter $g_0=cx_0$ (which gives the maximum value of the GF) on \hbar . It was found that g_0 monotonically decreases as \hbar increases (see Fig. 6); instead, the dependence of x_0 on \hbar is much less regular. The decrease of the value g_0 is consistent with the idea put forward in [8, 9] that quantum effects in the FK model may be accounted for by a reduction of the *kick strength* of the Standard map; anyway a more important quantum modification is given by the change of the GF to a sawtooth function.

For values of K not too much above K_{cr} (for example $K \sim 2$) the sawtooth function has to be replaced by some piecewise linear function obtained by connecting the

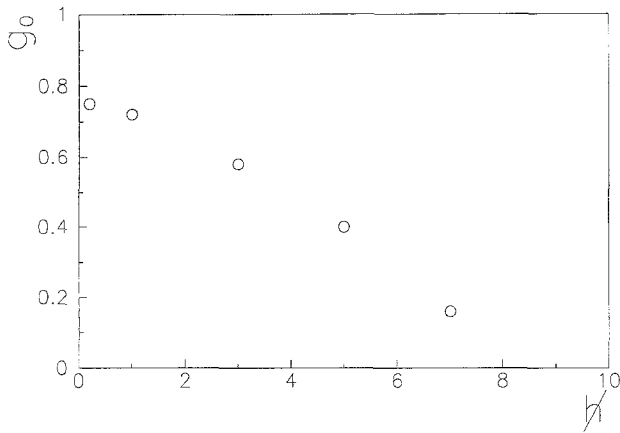


Fig. 6. Amplitude of the sawtooth map as a function of \hbar : plot of $g_0 = cx_0$ as defined in (3.1) vs. \hbar , for $\nu = 34/55$, $K = 5$

points of the Classical Cantorus by straight lines. Nevertheless the shape of the sawtooth function is practically the same for all $K > 4$.

As \hbar is increased, the steps in the QHF are more and more smoothed, and the QHF comes closer and closer to the diagonal [10]. In such deeply quantum regimes, the classical transition is completely effaced by quantum fluctuations.

In order to check that the above described picture is not just an outcome of the relatively small number

of oscillators, we made additional computations with $\nu = 89/144$ and $\nu = 233/377$. The obtained data are shown in Fig. 7 and demonstrate the independence of our results on the number of oscillators.

For K below K_{cr} the situation is quite different. The quantum GF is approximately sine-shaped, like the classical one, but its amplitude decrease as \hbar is increased, at least for not too large \hbar ($\hbar \sim 1$ for $K \sim 0.5$). The numerical analysis for larger \hbar becomes very difficult, because the decrease of temperature demands for a larger number of time steps.

4. Dependence of energy on temperature

In this last section we investigate the dependence of the energy of the quantum chain on temperature. Plots of the average energy per oscillator in the quantum model versus the temperature in the overcritical region are shown in Fig. 8. The numerical data were obtained by the Metropolis algorithm; in computing the average kinetic energy, the Feynman's prescription was used [11].

Typically these curves exhibit a plateau for small temperature and a linear growth (with unitary slope) for high temperature. The latter feature agrees with the classical predictions. Instead, the initial plateau appears to be connected with the classical phonon gap, which

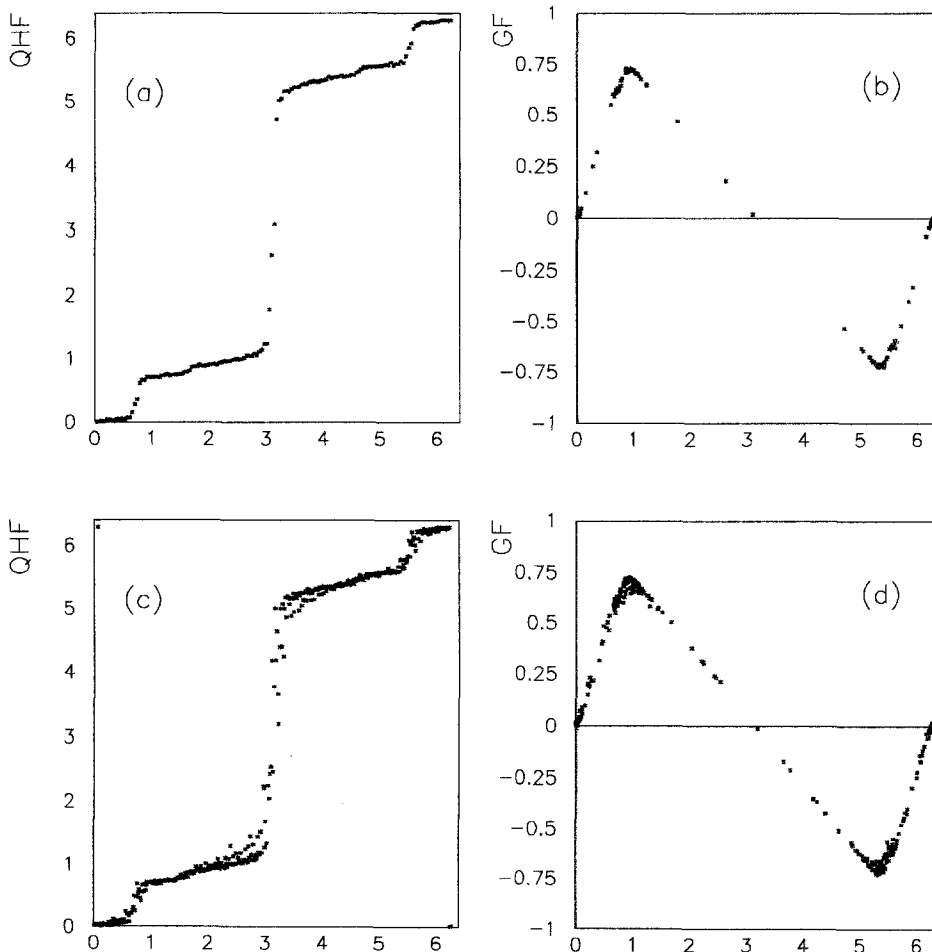


Fig. 7a-d. Quantum hull function (left) and g -functions (right) for $\hbar = 0.2$, $K = 5$. **a** and **b**: rotation number $\nu = 89/144$, **c** and **d**: $\nu = 233/377$

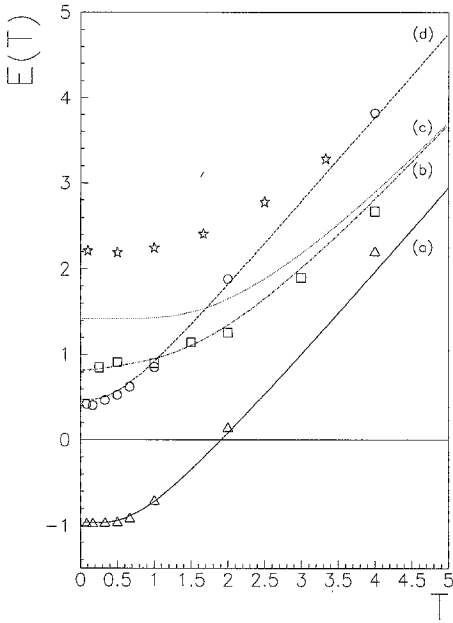


Fig. 8 a-d. Average energy per oscillator E vs. temperature T for winding number $\nu = 34/55$. The lines give $E(T)$ for the linearized chain, the symbols are Metropolis data for the actual chain. Triangles and full line **a**: $\hbar = 1$, $K = 5$. Circles and dashed line **d**: $\hbar = 1$, $K = 2$. Squares and dotted line **c**: $\hbar = 3$, $K = 5$. Stars: $\hbar = 5$, $K = 5$. The dashed and dotted line **b** is obtained from the sawtooth approximation with a fitting additive constant

sets a lower bound to the temperature required for significant excitation above the ground state. A more precise theoretical description of this effect was obtained by linearizing the classical model around the equilibrium configuration. In this way a system of harmonic normal modes was obtained. The spectrum of frequencies ω_i of these modes (the phonon spectrum) is shown in Fig. 9. In order to obtain an analytical expression for the dependence of the energy E on the temperature T , we quantized this system of phonons, and we used the Bose-Einstein formula for the average energy:

$$E(T) = E_0 + \sum_{i=1}^{s-1} \left(\frac{1}{2} \hbar \omega_i + \frac{\hbar \omega_i}{e^{\hbar \omega_i/T} - 1} \right) \quad (4.1)$$

where

$$E_0 = \sum_{i=1}^s \frac{1}{2} (x_{i+1}^e - x_i^e)^2 - K \sum_{i=1}^s \cos(x_i^e) \quad (4.2)$$

and x_i^e are the equilibrium positions for the classical model at zero temperature. The dependence of energy on temperature given by (4.1), for different values of K and \hbar , is shown by the smooth lines in Fig. 8. For small values of \hbar the agreement is quite good, but for large values of \hbar the law (4.1) does not fit any more the Metropolis data (see curve (c) on Fig. 8). This is probably due to the fact that for large \hbar the ground state structure changes as we have shown in previous section. Nevertheless the failure of this theoretical curve, based on the

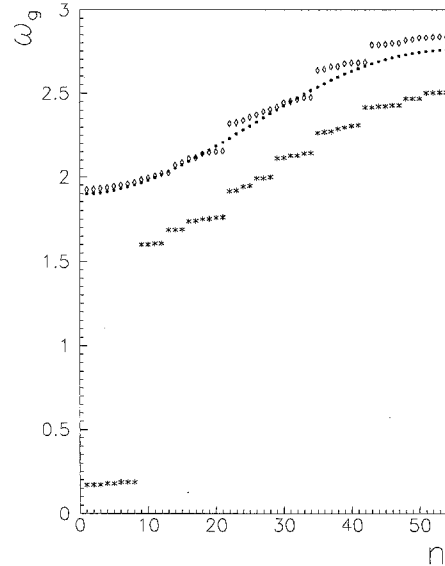


Fig. 9. Phonon spectrum. Classical phonon spectra for linearized motion, for $\nu = 34/55$, $K = 5$. Lozenges from linearizing the classical motion around the equilibrium positions as given by the Standard map. Asterisks from linearization around the equilibrium positions, as given by the sawtooth map obtained from Fig. 5 b, with parameters $x_0 = 1.2$, $c = 0.48$ corresponding to $\hbar = 3$ (see Eq. (3.1)). Dots from the sawtooth map obtained from Fig. 5 a with parameters $x_0 = 1$, $c = 0.72$ corresponding to $\hbar = 1$. ω_g is the frequency, n is the wave number

linearized motion near classical equilibrium positions, occurs for larger values of \hbar than would be expected on the grounds of the results of Sect. 3. For example that curve acceptably works even for values of \hbar for which significant changes of the GF could be observed (compare Fig. 1 f with 5 a). A qualitative explanation of this relatively good agreement may be provided by the fact that for the case with $\hbar = 1$ the number of points which deviate from the sine curve is relatively small and therefore does not lead to a significant change in energy.

On the other hand, a possible way for extending the validity of (4.1) to larger values of \hbar is suggested by the results of Sect. 3, which show that for large \hbar the ground state configuration is approximately described by a sawtooth map. This suggests that for such values of \hbar the phonon spectrum should be computed in a different way, namely by linearizing an “effective Hamiltonian” constructed in such a way that its equilibrium positions are given by the sawtooth map. This effective Hamiltonian is determined by the sawtooth function obtained from the quantum GF, apart from an additive constant, which we used as a fitting parameter in our computations.

The phonon spectrum determined in this way is shown in Fig. 9. By this method a satisfactory agreement with Metropolis data was obtained (see curve (b) on Fig. 8). Moreover, for $\hbar < 1$, the phonon spectra obtained from the Standard map and from the sawtooth map agree with each other (see Fig. 9), and this yields another explanation of the good fitting of the Metropolis data

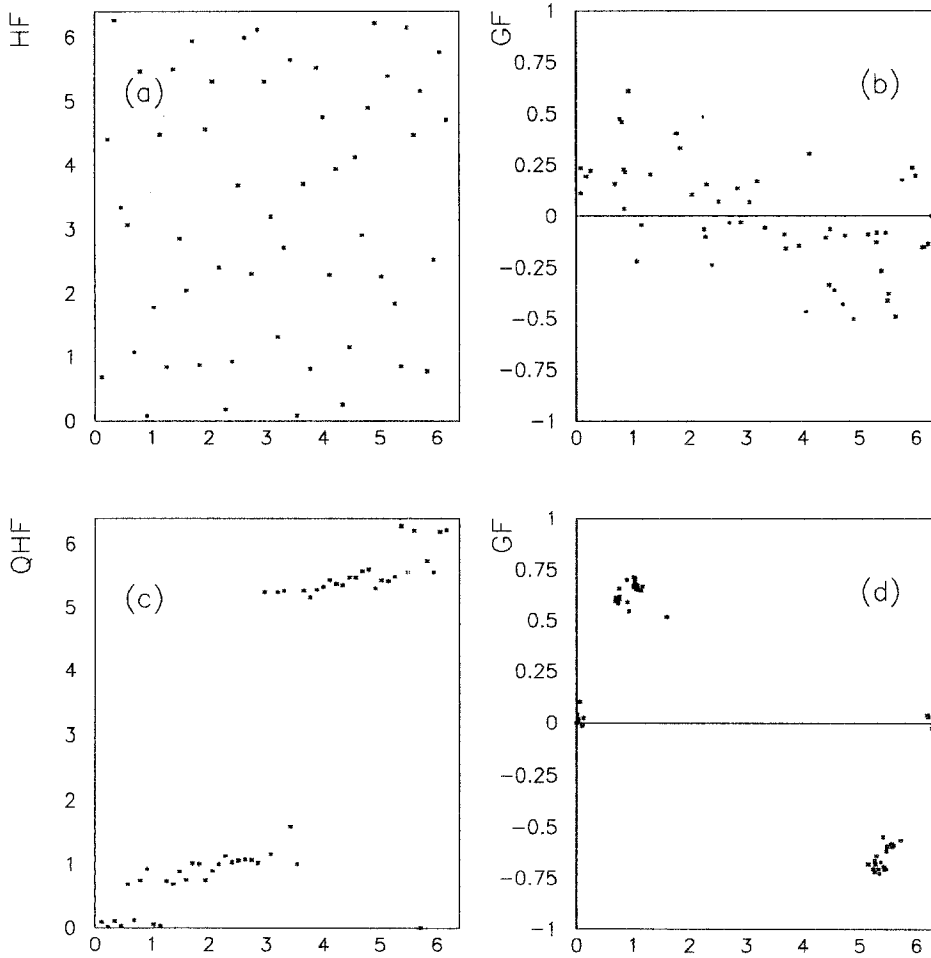


Fig. 10a-d. Comparison between quantum and classical hull-function and g -function at the same finite temperature $T=0.5$. The parameters are $K=5$, $\nu=34/55$. **a** Classical “hull-function”, **b** Classical “ g -function”; **c** Quantum hull-function; **d** Quantum g -function

by means of formula (4.1) with the original phonon spectrum ω_i .

The parameters of the sawtooth map depend on \hbar as illustrated in Fig. 5. Therefore, the phonon spectrum associated with that map must be expected to change with \hbar , too. As a matter of fact, Fig. 9 clearly shows that the phonon gap undergoes a sharp reduction as \hbar increases from 1 to 3. It is interesting to analyze this phenomenon in the light of some rigorous mathematical results on the sawtooth map available in the literature [17]. According to these results no invariant curves exist at all when *

$$g_0 > g_{\text{cr}} = \frac{4}{K} \frac{(\pi - x_0)^2}{2\pi - x_0}. \quad (4.3)$$

From (4.3) we obtain for $x_0 = 1$, $K = 5$, (which correspond to $\hbar = 1$): $g_{\text{cr}} = 0.695$. This is less than $g_0 \approx 0.72$ numerically obtained from the quantum case, so that no invariant curves for the sawtooth map should exist and a nonzero phonon gap should be expected. On the other hand the difference between these two values is quite small, and quantum fluctuations make it difficult to decide whether the Quantorus is better described by an invariant curve or by a Cantorus.

* The connection between our parameters and the parameters k , a used in [17] is the following: $k = Kg_0/(\pi - x_0)$; $a = (1/2 - x_0/2\pi)$

In the other case of Figs. 9 for $x_0 = 1.2$, $K = 5$ ($\hbar = 3$) we have $g_{\text{cr}} = 0.593$ which is now larger than the numerical value $g_0 \approx 0.57$ obtained from the quantum model. Formula (4.3) does not any more exclude that invariant curves for the sawtooth map exist, and this would qualitatively agree with the strong decrease of the phonon gap observed in this case. This qualitative argument is however not conclusive, because the critical value of g_0 at which all invariant curves with a given rotation number ν disappear depends on ν in a peculiar fractal way [17] and we do not actually know the exact critical value for our rotation number. Anyway, on account of the smallness of the phonon gap we can assume the Quantorus to be closer to an invariant curve than in the previous case with $\hbar = 1$.

Another interesting feature of the phonon spectrum (for $\hbar = 3$) associated with the sawtooth map is the small value of the first and second derivative ($v_g = d\omega_g/dn \sim 0$, $1/M = d^2\omega_g/dn^2 \sim 0$). This behaviour is qualitatively different from that of the linear phonon spectrum both in the case of invariant curves ($v_g = \text{const} > 0$), and in the case of Cantori ($1/M > 0$). This property, which appears to correspond to a quasiparticle with a very large mass M , can be connected with the unusual property of the sawtooth map of having invariant curves even for some rational rotation numbers.

It is also worth mentioning that classical thermal

effects affect the FK model in quite a different way than quantum effects do. In the first place the dependence of energy on temperature in the undercritical as well as in the overcritical case follows, for $T > 0.01$, a straight line of unitary slope, while in the quantum case we have practically no change of energy for temperature less than $\hbar\omega_g/2$, where ω_g is the phonon gap (see Fig. 8). The conclusion that the Quantum and the Classical FK model at the same temperature display quite different properties is also enforced by more detailed data [18]. For example, a comparison of g -function and hull-functions (Fig. 10) shows that while the quantum characteristics are still close to the ground state ones, in spite of the nonzero temperature, the classical g -function and hull-function are completely destroyed.

A final remark is that the existence of the phonon gap facilitates the quantum numerical investigation of the ground state, because in this case there is a significant distance between the ground state and the first excited state. For this reason, it is not necessary to use so small temperatures as would be required in the undercritical case.

5. Conclusions

In this paper we have reported about results of extensive numerical simulations on the quantum Frenkel-Kontorova model. These results illustrate how the characteristics of the quantum ground state reflect the sharp transition which takes place in the classical model at a critical value of the parameter, and provide evidence that, at least for not too large \hbar , a crossover in the nature of the quantum ground state occurs, somehow mimicking the classical transition. A more physical evidence of this crossover is given by the behaviour of the quantum energy as a function of temperature. We emphasize that in the overcritical regime an important modification appears in the quantum ground state average positions of the oscillators, which are described by a sawtooth map instead of the Standard map.

The bulk of the above reported investigations was aimed at analyzing the effects of quantum fluctuations on the Cantori structure which characterize the classical ground state in the overcritical regime. Our results give for the first time some precise indication in this sense, beyond the obvious intuition that the classical structure

should be somehow blurred. Though these indications are very far from the standard of mathematical precision of the classical theory of the FK model, we believe that they may provide useful hints in connection with the general problem of the relevance of classical Cantori in quantum mechanics.

We are grateful to B.V. Chirikov for interesting discussions. This work was partially realized according to the CNR (Italy) – Academy of Sciences (USSR) agreement.

References

1. Eckhardt, B.: Phys. Rep. **163**, 205 (1988)
2. Mackay, R.S., Meiss, J.D., Percival, I.C.: Physica **13D**, 55 (1984)
3. Aubry, S.: Physica **7D**, 240 (1983)
4. Aubry, S., Daeron, P.Y.: Physica **8D**, 381 (1983)
5. Chirikov, B.V., Shepelyansky, D.: Radiofizika **29**, 1041 (1986)
6. Geisel, T., Radons, G., Rubner, J.: Phys. Rev. Lett. **57**, 2883 (1986)
7. Pokrovsky, V.L., Talapov, A.L.: Theory of incommensurate crystals. Sov. Sc. Rev. Suppl. Series Phys. V.1 (1984)
8. Berman, G.P., Iomin, A.M.: Phys. Lett. **107A**, 324 (1985); Zh. Eksp. Teor. Fiz. **89**, 946 (1985)
9. Beloshapkin, V.V., Berman, G.P., Iomin, A.M., Tret'yakov, A.G.: Zh. Eksp. Teor. Fiz. **90**, 2077 (1986)
10. Borgonovi, F., Guarneri, I., Shepelyansky, D.: Phys. Rev. Lett. **63**, (No. 19), 2010 (1989)
11. Creutz, M., Freedman, B.: Ann. Phys. **132**, 427 (1981)
12. Shuryak, E.V., Zhirov, O.V.: Nucl. Phys. B **242**, 393 (1984)
13. Chirikov, B.V.: Phys. Rep. **52**, 263 (1979)
14. Greene, J.M.: J. Math. Phys. **20**, 6 (1979)
15. Mackay, R.S.: Physica **7D**, 283 (1983)
16. Peyrard, M., Aubry, S.: J. Phys. C **16**, 1593 (1983)
17. Bullett, S.: Commun. Math. Phys. **107**, 241 (1986)
18. Borgonovi, F.: Ph. D. Thesis, Università di Pavia (Italy) (in preparation)

F. Borgonovi^{1,2}, I. Guarneri¹, D. Shepelyansky²

¹ Dipartimento di Fisica Nucleare e Teorica dell'Università di Pavia and Istituto Nazionale di Fisica Nucleare
Via Bassi 6
I-27100 Pavia
Italy

² Institute of Nuclear Physics
SU-630090 Novosibirsk
USSR